 doi:10.20944/preprints202208.0076.v1

Article

Semi-analytical lower-bound limit analysis of domes and vaults

Renato Zona [1,‡], Luca Esposito [2,‡], Simone Palladino [3,‡], Elena Totaro [4,‡] and Vincenzo Minutolo [5,*]

[1] Department of engineering University of Campania "L.Vanvitelli", Italy; renato.zona@unicampania.it
[2] Department of engineering University of Campania "L.Vanvitelli", Italy; luca.esposito@unicampania.it
[3] Department of engineering University of Campania "L.Vanvitelli", Italy; simone.palladino@unicampania.it
[4] Department of engineering University of Campania "L.Vanvitelli", Italy; elena.totaro@unicampania.it
[5] Department of engineering University of Campania "L.Vanvitelli", Italy; vincenzo.minutolo@unicampania.it
* Correspondence: vincenzo.minutolo@unicampania.it
‡ These authors contributed equally to this work.

Featured Application: The possible application of the work is in the forecast of the stability of masonry structures or concrete structures. The result is very useful for addressing the restoration and to interpret the results of experimental monitoring of the structures during their time-life. The non linear analysis made by means of the upper bound theorem of the limit design allows evaluating the response to different randomly variable and unknown load paths giving the overall safety factor. In this way, real life behavior of the structures can be addressed form practitioners that have to monitor and restore the art crafts.

Abstract: The calculation of the collapse load of spherical domes is addressed using a semi-analytical approach under the hypotheses of small displacements and perfect plasticity. The procedure is based on the numerical approximation of the self-stress that represents the projection of the balance equilibrium null space on a finite dimensional manifold. The so obtained self-equilibrated stress span is superimposed to a finite element linear elastic solution to the prescribed loads yielding to the statically admissible set accordingly to Melan's theorem. The compatibility of the stress with the constitutive law of the material has been enforced using linearized limit domain in terms of generalized stress, namely axial force and bending moment along the local spherical curvilinear coordinates. The procedure has been tested with reference to numerical and experimental data from the literature confirming the accuracy of the proposed method. The comparison with the literature confirms that the buckling load is much greater than the plastic collapse loads both calculated through the proposed procedure and reported in the quoted literature.

Keywords: Limit analysis of domes; Concrete caps; experiment comparison; Not Tensile Resistant Materials ; Finite element

1. Introduction

The spherical shell safety to applied loads is related to the loss of equilibrium consequent to geometric or constitutive limits attainment. The geometric limit trespass consists of the buckling or the snapping phenomenon insurgence whilst the constitutive limits involves the plastic collapse of the structure. The two phenomena are connected since plastic collapse occurs when the buckling limit is attained because of the great stress level consequent to large deflections arising when the structure buckles, analogously, the buckling occurs when, due to plastic collapse, large deflections appear. Combined limit evaluation implies coupled formulation that can generally be resolved only through path following analysis. In the following, we refers to limit analysis only in order to get the collapse loads and mechanisms under the hypotheses of small displacements plasticity. To calculate the limit load for plastic collapse of the structures the limit analysis results one of the tools that received major interest in time. Recently, static analysis obtained renewed interest in the masonry structures framework due to the trust-line method and limit equilibrium application [1–4]. The limit analysis is used for the safety assessment of concrete domes and aches for large structures as shown in [5–7]. In particular, [8,9]

 doi:10.20944/preprints202208.0076.v1

investigates concrete vessels' composite structures considering collapse and buckling loads evaluation. In [10] an application of the kinematic method is presented for the first order assessment strategy of the structure safety. Size effects and corresponding influence on the structural limit behavior is addressed in a different manner by the work [11] considering domes stability under spreading supports. experimental and analytical results using limit analysis are presented in [12], where the results are compared with those obtained from the experimental campaign reported in [13]. In particular the work [12] highlights that the collapse load of concrete caps is calculated through crack lines development balance using an analytical formulation that applies the upper-bound kinematic approach of the limit analysis; moreover, the collapse formula is compared to the experimental campaign from [13] and to the buckling load calculated in [14] and the accuracy of the proposed limit analysis is addressed. In particular the work [12] reports that the collapse load from experimental campaign is predicted by the limit analysis rather than buckling theoretical formulas. In the references of paper [15–17] a more comprehensive literature can be found.

In the present paper, we discuss an application of the semi-analytical formulation that presents the lower bound theorem of the limit analysis to assess domes' collapse load based on the self-equilibrated solution of the balance equations. The present work has been devoted to apply the procedure that is reported in [15,17] to slender concrete caps already studied by [13] with the scope of comparing the proposed semi-analytical formulation to the experiments and the theoretical formulation from [12]. The limit analysis lower-bound proposed formulation is rather general, it can deals with any structure for which analytical balance equation exists and can be solved numerically for calculating the self-equilibrated stress set. The load can vary in time both monotonically and randomly, provided the time variation is slow enough to prevent inertial effects. The procedure recalls the Melan's theorem hence it requires the knowledge of the linearly elastic solution due to the applied loads. Such an elastic solution has been obtained through homemade APDL routine written for finite element program ANSYS© Multiphysics (ANSYS Inc., Canonsburg, PA, USA). The use of the finite element to obtain the elastic solution allows to free the particular solution from the knowledge of the actual elastic stress. The compatibility condition has been formulated accordingly to Melan's theorem in the stress space [18], and the eigen-solution has been discretized to be handled in a numerical optimization program that finds the load multiplier. The results from the proposed formulation showed a good agreement with the experiments done by Vandepitte and Lagae [13] and with analogous calculation presented by [12,19] that has been obtained with a somewhat different application of the limit analysis formulated in terms of collapse lines and upper bound theorem.

In the work, starts from a brief outline of the general formulation is reported. At first, the spherical domes equilibrium equations have been recalled, and the eigen-solution, i.e., the solution of the homogeneous equation, in discretized form has been introduced. In the subsequent section, the constitutive and compatibility equations of the unreinforced concrete that constitutes the caps' material have been described, and the limit domain has been derived in linearized form. Furthermore, the case study has been presented and the linear elastic solution derived using finite element linear analysis has been presented. Finally, the optimization program used to get the collapse load multiplier has been described and results discussed. It has been shown that the result depends on the parameters of the eigen-solution, that was the design variables, that represent the Melan's residuals of the structure at the incoming collapse.

2. Equilibrium and self-equilibrium of domes

This section briefly recalled a spherical shell equilibrium equation, the complete treatment can be found in [20]. The formulation have used the generalized stress as mechanical parameters, hence the stress has been described through the internal forces, N, T, and M that are the resultant components, axial and shear forces respectively, and the resultant bending moment of the stress acting on the section, see Fig.1. Only the axial force and bending moment are assumed to influence the structure's safety since the shear

Preprints (www.preprints.org) | NOT PEER-REVIEWED | Posted: 3 August 2022 doi:10.20944/preprints202208.0076.v1

effects are negligible due to the small thickness of the caps. The internal forces are statically equivalent to a single one of magnitude N acting on point C called the center of thrust of the section. The line connecting all the centers along the structure's axis is called the structure's thrust line, depending on the actual load condition.

The procedure that follows has been widely described in [15,17]. The solution of the homogeneous form of the balance equations represents the domain of the eigen-stress of the shell. The set of equilibrium equations of a spherical dome has the following expression with the symbols summarized in the drawings in Fig.3:

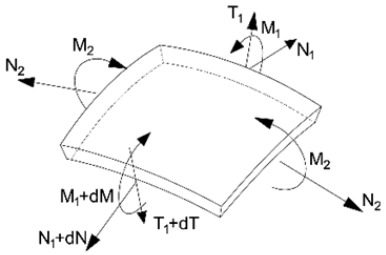

Figure 1. Stress resultants on the dome infinitesimal element

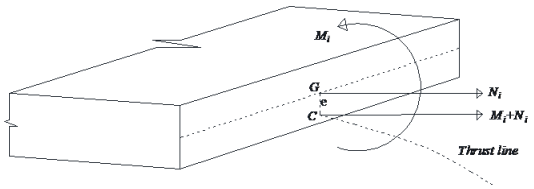

Figure 2. Center of thrust at a cross section

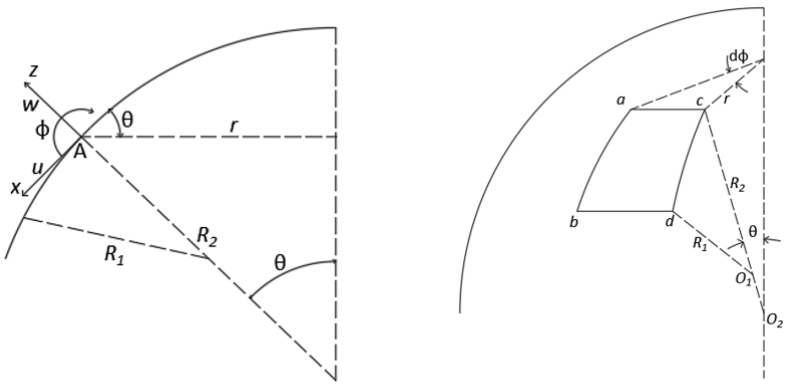

a) b)

Figure 3. Geometric parameters (a), infinitesimal element of the dome (b)

$$\begin{cases} \frac{d(N_1R_1sin\theta)}{d\theta} - N_2R_1cos\theta - T_1R_1sin\theta & = -XR_1^2sin\theta \\ N_1R_1sin\theta + N_2R_1sin\theta + \frac{d(T_1R_1sin\theta)}{d\theta} & = ZR_1^2sin\theta \\ \frac{(M_1R_1sin\theta)}{d\theta} - M_2R_1cos\theta - T_1R_1^2sin\theta & = 0 \end{cases} \quad (1)$$

Due to the symmetry of the loads and shell, the stress depends only on the co-latitude angle θ. Hence, the self-equilibrated generalized stress set $\mathcal{C} = \{N_1^0, M_1^0, T_1^0, N_2^0, M_2^0\}$ satisfies the following equations:

Preprints (www.preprints.org) | NOT PEER-REVIEWED | Posted: 3 August 2022 doi:10.20944/preprints202208.0076.v1

$$\begin{cases} \frac{d\left(N_1^0 r\right)}{d\theta} - N_1^0 R_1 cos\theta - T_1^0 r = 0 \\ N_1^0 r + N_1^0 R_1 sin\theta + \frac{d\left(T_1^0 r\right)}{d\theta} = 0 \\ \frac{d\left(M_1^0 r\right)}{d\theta} - M_2^0 R_1 cos\theta - T_1^0 R_1 r = 0 \end{cases} \tag{2}$$

A set of polynomial shape functions of degree n is used to the numerical approximation of the solution of equation (2).

$$S_n(\theta) = \left[\theta^0, \theta^1, .., \theta^n / n!\right] \tag{3}$$

whose derivatives are:

$$dS_n(\theta) = \left[0, 1, \theta, ..., \frac{\theta^{n-1}}{(n-1)!}\right] = [0] \cup S_{n-1}(\theta) \tag{4}$$

Five nodal parameters sets are used to approximate the unknown five self-equilibrated stresses. Using the same approximation for all the stress functions the following expressions result:

$$\begin{cases} N_1^0 &= S_n(\theta)\mathbf{N_1} \\ N_2^0 &= S_n(\theta)\mathbf{N_2} \\ M_1^0 &= S_n(\theta)\mathbf{M_1}, \\ M_2^0 &= S_n(\theta)\mathbf{M_2} \\ T_1^0 &= S_n(\theta)\mathbf{T_1} \end{cases} \begin{cases} \mathbf{N_1} &= [n_{10}, n_{11}, ..., n_{1n}]^T \\ \mathbf{N_2} &= [n_{20}, n_{21}, ..., n_{2n}]^T \\ \mathbf{M_1} &= [m_{10}, m_{11}, ..., m_{1n}]^T, \\ \mathbf{M_2} &= [m_{20}, m_{21}, ..., m_{2n}]^T \\ \mathbf{T_1} &= [t_{10}, t_{11}, ..., t_{1n}]^T \end{cases} \begin{cases} \frac{d\left(N_1^0 r\right)}{d\theta} = dS_n(\theta)\mathbf{N_1} \\ \frac{d\left(N_2^0 r\right)}{d\theta} = dS_n(\theta)\mathbf{N_2} \\ \frac{d\left(M_1^0 r\right)}{d\theta} = dS_n(\theta)\mathbf{M_1} \\ \frac{d\left(M_2^0 r\right)}{d\theta} = dS_n(\theta)\mathbf{M_2} \\ \frac{d\left(T_1^0 r\right)}{d\theta} = dS_n(\theta)\mathbf{T_1} \end{cases} \tag{5}$$

By substituting equations (5) into equation (2) and collecting the unknown parameters in a single vector $\mathbf{x} = [\mathbf{N_1}, \mathbf{N_2}, \mathbf{M_1}, \mathbf{M_2}, \mathbf{T_1}]$, the self-equilibrium equations can be rewritten in compact matrix form:

$$\mathbf{Ax} = \mathbf{0} \tag{6}$$

where $\mathbf{A}$ is:

$$\mathbf{A}(\theta) = \begin{bmatrix} \left(\frac{dr}{d\theta} S_n(\theta) + r dS_n(\theta)\right) & -S_n(\theta) R_1 cos(\theta) & 0 & 0 & -r S_n(\theta) \\ r S_n(\theta) & S_n(\theta) R_1 cos(\theta) & 0 & 0 & \frac{dr}{d\theta} S_n(\theta) + r dS_n(\theta)) \\ 0 & 0 & \frac{dr}{d\theta} S_n(\theta) + r dS_n(\theta)) & -S_n(\theta) R_1 cos(\theta) & -r S_n(\theta) \end{bmatrix} \tag{7}$$

Equation (6) has no unique solution since the number of the unknowns is greater than the number of equations. Consequently, it is possible to find only three of the unknown variables as a function of the $5n - 3$ leftover ones, represented by the vector $\mathbf{c}$, namely the basis that spans the set of self-equilibrated stress:

The solution of equation (6) has been expressed in terms of $\mathbf{c}$ and introduced into the relationships (5) giving the stress:

$$\begin{pmatrix} \mathbf{N}_1^0 \\ \mathbf{N}_2^0 \\ \mathbf{M}_1^0 \\ \mathbf{M}_2^0 \\ \mathbf{T}_1^0 \end{pmatrix} = \begin{pmatrix} \mathbf{K}_{N1}^0 \\ \mathbf{K}_{N2}^0 \\ \mathbf{K}_{M1}^0 \\ \mathbf{K}_{M2}^0 \\ \mathbf{K}_{T1}^0 \end{pmatrix} \mathbf{c} \tag{8}$$

where the matrices $\mathbf{K}_{N1}^0$,$\mathbf{K}_{N2}^0$,$\mathbf{K}_{M1}^0$,$\mathbf{K}_{M2}^0$, and $\mathbf{K}_{T1}^0$ collect the shape functions reassembled to fulfill the solution of the equation (6).

Preprints (www.preprints.org) | NOT PEER-REVIEWED | Posted: 3 August 2022 doi:10.20944/preprints202208.0076.v1

3. Constitutive equations

The constitutive equation governs the compatibility constraints of the optimization program that calculates the limit load multiplier. In the actual application we refers to Not Tensile Resistant (NTR) material, namely the uni-axial tensile strength σ_t^0 is:

$$\sigma_t^0 = 0 \tag{9}$$

and the compression strength limit σ_c^0 belongs to the bounds

$$-\infty \leq \sigma_c^0 < 0 \tag{10}$$

where the lower-bound limit $\sigma_c^0 = -\infty$ corresponds to the hypothesis of Heyman [21].

The limit domain has been derived for the rectangular cross-section with unit width of the concrete cap. The limit domain has been described in terms of the generalized stress, N and M considering that the Bernoulli's hypotheses of plane cross section holds true as in [19]. The compression strength has been considered finite, and the admissible domain has been obtained by the balance equation about the neutral axis of the section. It has furnished the limit bending moment for any coupled axial force. The domain has been described by the two relations giving the bending moment as a function of the axial force.

$$M = \mp \frac{N(N - bh\sigma_c^0)}{2b\sigma_c^0} \tag{11}$$

where h and b are the height and the width of the section, respectively. The Fig.4 shows the resulting domain obtained using the data reported in [19].

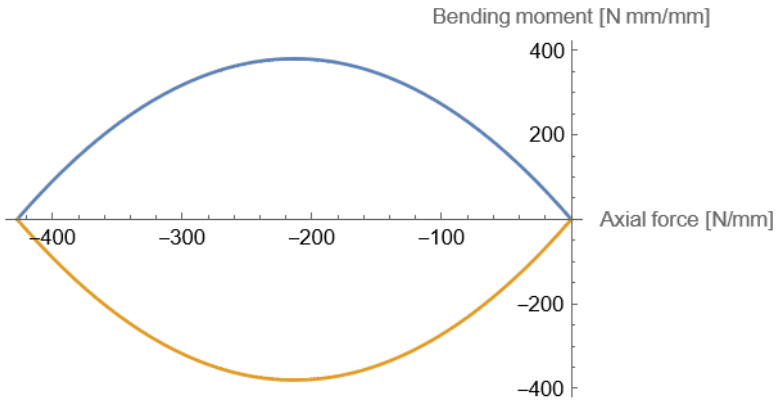

Figure 4. Caps' limit domain per unit width cross section, blue and orange curves correspond to +/- sign in Equation (11).

The limit domain governs the compatibility constraints of the optimization program that furnishes the collapse load multiplayer. In the following, a linear programming technique has been employed. Consequently, a linearization of the domain has been introduced. Starting from the maximum bending moment M_y, in absolute value, that corresponds to the stationary points of the domain boundary curves in Fig.4, four linear interpolation of the curved domain has been obtained. The set of linearized inequalities that represent the limit domain approximation are:

$$\begin{cases} M < -\frac{h}{4}N \\ M > \frac{h}{4}N \\ M < +\frac{h}{4}N + 2M_y \\ M > -\frac{h}{4}N - 2M_y \end{cases} \tag{12}$$

In Fig.5, the shape of the linearized domain is depicted.

Preprints (www.preprints.org) | NOT PEER-REVIEWED | Posted: 3 August 2022 doi:10.20944/preprints202208.0076.v1

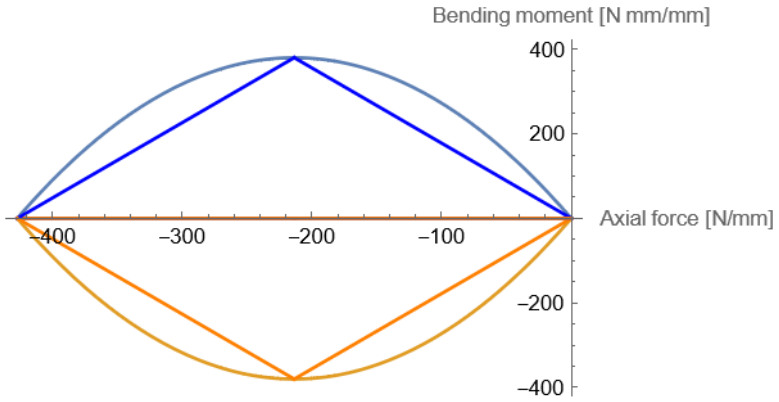

Figure 5. Linearization of the limit domain, blue and orange curves correspond to sign in equation (11)

Following Melan's theorem, the limit multiplier of prescribed load paths, either monotonically increasing or randomly varying, is obtained by maximizing the load multiplier under the constraint that the sum of the elastic response to the loads and a self-equilibrated time-independent stress belongs to the admissible domain. The procedures consists of a constrained maximum research where the objective function is the load multiplier. The optimization constraints are the linear inequalities (12). It has to note that the linearized domain is a proper subset of the original one. Consequently, the admissible stress state satisfying the linearized compatibility constraint constitutes an admissible stress state for the nonlinear domain too. The numerical results have been obtained introducing the self equilibrated solution (8) have been collocated on discrete points of the domes corresponding to a mesh of parallels and meridians that has been individuated. The same mesh has been used to get the elastic solution and the collocation points of the representation (5) of the self-equilibrated solution. The case study concerned axial symmetrical structure under axial symmetrical loads so that only one meridian has been studied where a finite number of the co-latitude angle has been set.

The constrained maximum program has the following numerical form:

$$\underset{\mathbf{c}}{sup}\, k \left| k \in R^{+} : \begin{cases} 4(M^{0}_{ij} + kM^{e}_{ij}) \leq -h(N^{0}_{ij} + kN^{e}_{ij}) \\ 4(M^{0}_{ij} + kM^{e}_{ij} \geq h(N^{0}_{ij} + kN^{e}_{ij}) \\ 4(M^{0}_{ij} + kM^{e}_{ij}) \leq h(N^{0}_{ij} + kN^{e}_{ij}) + 8M_{y} \\ 4(M^{0}_{ij} + kM^{e}_{ij}) \geq -h(N^{0}_{ij} + kN^{e}_{ij}) - 8M_{y}) \end{cases} \right|^{j} \tag{13}$$

In the program (13), N^{e}_{ij}, M^{e}_{ij} are the elastic solution and N^{0}_{ij}, M^{0}_{ij} are the self-equilibrated stress, the subscript "i" refers to the discrete angles, θ_i where the inequalities in (13) have been collocated that define the sampling point set and "$j = 1, 2$"corresponding to the meridian or parallel directions,see Fig.1. The formulation (13) has a general form since the representation of the self-equilibrated stress in complete for the structures described by equations (1). The elastic solution characterize the load applied on the domes hence very general load case, provided it is axial-symmetrical, can be applied. Consequently, the method demonstrates its valuable advantage compared to the step-by-step numerical method and is more general than simply analytical methods calculating collapse loads using analytical closed-form approaches. The proposed method seems to have the simplicity that suggests using it for evaluating directly the collapse load joined with the generality due to the possibility of handling rather complicated load time histories both monotonically or randomly variable.

Preprints (www.preprints.org) | NOT PEER-REVIEWED | Posted: 3 August 2022 doi:10.20944/preprints202208.0076.v1

4. Case Study: Concrete Caps Collapse Load

To validate the method with the respect to experimental data, a numerical campaign has been developed. The analysis has concerned slender spherical domes, made of unreinforced concrete, clamped at the base, and loaded by uniform radial pressure. The concrete caps were calculated to obtain the limit uniform radial pressure triggering the collapse. The load program consisted of monotonically increasing radial pressure through a scalar multiplier k, superimposed to a fixed uniform self-weight. The calculation aims to search for the collapse value of k, say s_c, for which the compatibility conditions hold. The routine calculating the semi-analytical solution of the self-equilibrium equation has been implemented in Mathematica® (Wolfram, Champaign, IL, USA) environment. The structure's geometry has been obtained from [13] so that a comparison with experimental results could be made. In particular, several different domes have been calculated considering the reported experimental data where the slight differences in the shells' radius and thickness, strength, and elastic properties have been considered. The detailed dimensions of the specimens are reported in Table1

4.1. FEM elastic solution

The elastic response of the structures to the radial uniform pressure has been calculated numerically using the finite elements Ansys© program. The elastic solution has been collected in the matrix of elastic stresses containing the parameters $\boldsymbol{F}^* = \{\boldsymbol{N}^e_{ij}, \boldsymbol{M}^e_{ij}, \boldsymbol{T}^e_{i1}\}$ calculated at discrete points on the meridian curve, see Fig.6. The FEM results have been introduced into the semi-analytical procedure described by equation (13).

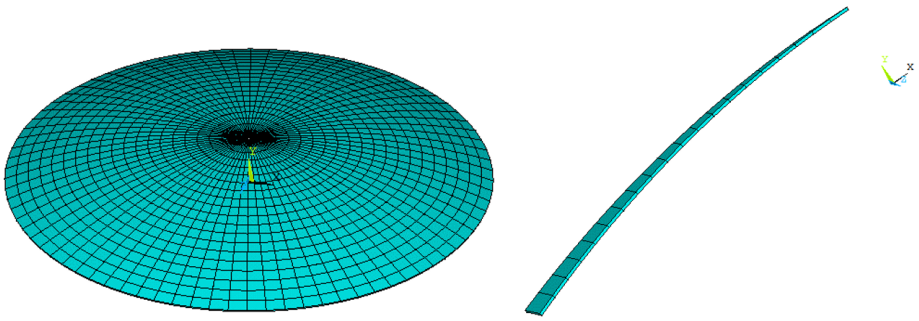

Figure 6. Cap discretization:a) Whole model; b) Single meridian element selection

The caps have been modeled using eight-node shell elements with 6 degrees of freedom for each node and quadratic shape functions. The axial forces and the bending moments acting on each shell element cross-section perpendicular to the parallels and meridians have been collected. The numerical finite element elastic solution and the semi-analytical self-equilibrated solution have been superimposed to obtain the statically admissible stress to introduce into the compatibility inequality constraints of the optimization program equation (13). The elastic solution has been obtained at little computational cost since only linear elastic solution has been calculated.

5. Results and discussion

The obtained results have been summarized in the Tab.1 where the literature results are reported as well. In particular for each specimen, besides to the identifier, the thickness and the radius of the dome, the compression stress limit, and the young modulus as reported in [13] and in [12,19] have been indicated. The results of the present analysis have been reported in comparison with the cited references. In particular, in the the table, the collapse multiplier from the experiments of Vandepitte and Lagae [13] (ex), the analytical value

Preprints (www.preprints.org) | NOT PEER-REVIEWED | Posted: 3 August 2022 doi:10.20944/preprints202208.0076.v1

of the buckling load from [14] (BL), the numerical results obtained through the collapse line mechanism reported in [19] (CL), and the collapse load obtained from the present Semi-Analytical Method (SAM) have been collected.

The SAM output consists of the load collapse multiplier, and of the Melan's residual stress representing the self equilibrated stress that summed to the elastic solution respects the compatibility constraints. Consequently it is possible to calculate the eccentricity, e of the Melan compatible stress as

$$e_{ij} = \frac{M^c_{ij}}{N^c_{ij}} \tag{14}$$

where M^c_{ij} and N^c_{ij} are the resulting stress from the optimization procedure.

The eccentricity is the distance along with the thickness of the cross-section of the center of trust C from the centroid of the section, hence the line connecting the eccentricity of the sections is the trust line of the structure at the incoming collapse. In Fig.7, the thrust line of the KN37 specimen meridian cross-section is reported together with the amplitude of the structure's core and thickness. It can be seen that such a line lies within the thickness of the structure. A three-dimensional representation of the trust locus is depicted in Fig. 8 for the same sample KN37.

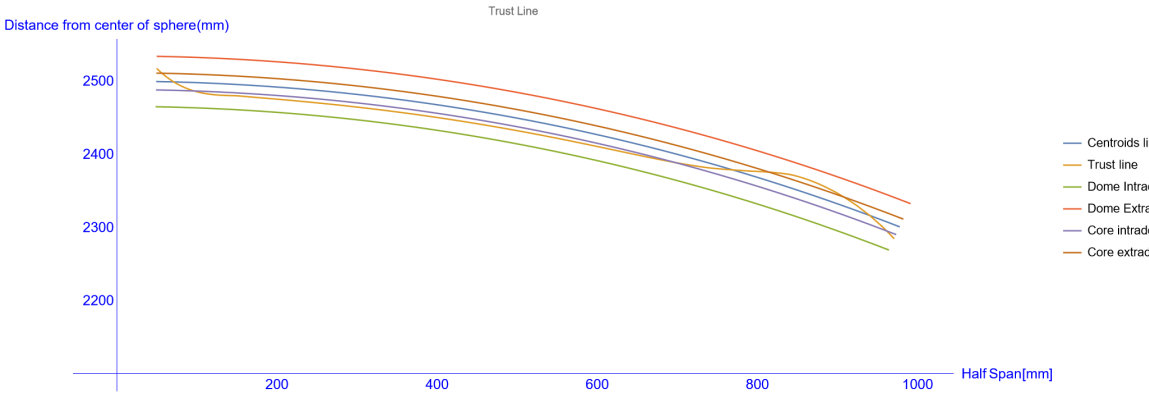

Figure 7. Thrust Line along with the meridian and thickness

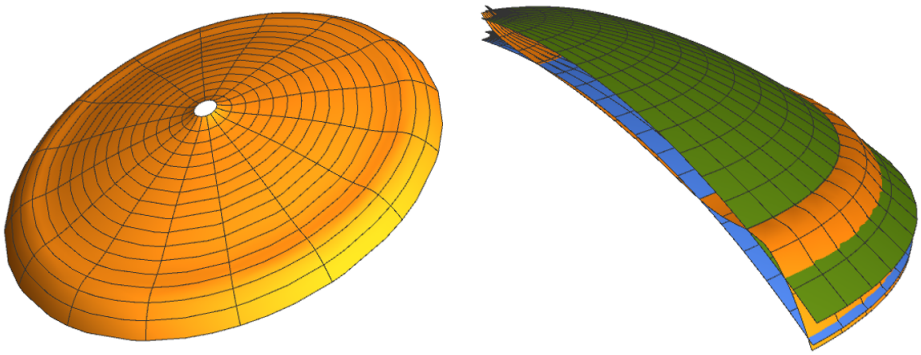

Figure 8. a) Three-dimensional representation of the locus of the centers of axial forces: the Thrust Surface, b) Axonometric section with the indication of the core thickness

Preprints (www.preprints.org) | NOT PEER-REVIEWED | Posted: 3 August 2022 doi:10.20944/preprints202208.0076.v1

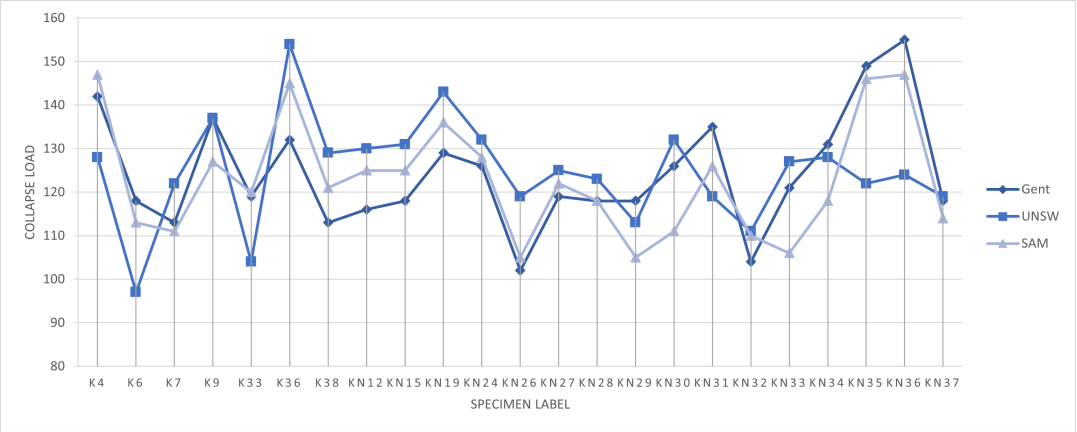

Figure 9. Collapse load from ex, (CL), and present SAM procedure

Table 1. Specimen data and results comparison.

tiny Specimen	Thickness	Radius	Strength	Young Modulus	(Ex)	BL	(CL)	SAM	(Ex)/SAM
K4	7.12	2431	60	30356	142	305	128	147	1.035
K6	7.07	2438	46	25667	118	254	97	113	0.958
K7	6.91	2428	59	22799	113	217	122	111	0.982
K9	6.98	2450	66	29013	137	276	137	127	0.927
K33	6.91	2469	51	33652	119	310	104	120	1.008
K36	6.9	2479	76	31527	132	286	154	145	1.098
K38	6.86	2524	65	29269	113	255	129	121	1.071
KN12	7.07	2538	64	26126	116	240	130	125	1.078
KN15	6.94	2554	66	26537	118	230	131	125	1.059
KN19	6.99	2537	71	34230	129	304	143	136	1.054
KN24	7.1	2560	65	32176	126	296	132	128	1.016
KN26	7.06	2546	59	26766	102	242	119	105	1.029
KN27	7.09	2557	62	30523	119	276	125	122	1.025
KN28	7.01	2540	61	30033	118	269	123	118	1
KN29	6.76	2535	58	31449	118	263	113	105	0.89
KN30	6.98	2515	58	32958	126	298	132	111	0.881
KN31	7.04	2500	65	33825	135	306	119	126	0.933
KN32	6.93	2500	58	26904	104	236	111	110	1.058
KN33	7.02	2500	55	26888	121	243	127	106	0.876
KN34	6.94	2500	62	28962	131	254	128	118	0.901
KN35	6.83	2500	63	34208	149	292	122	146	0.98
KN36	6.98	2500	61	34760	155	310	124	147	0.948
KN37	6.89	2500	61	33326	118	290	119	114	0.966

In the Fig.9, the comparison of different models and experiments is drawn as a function of the specimen identifier. It can be seen that the calculation from (CL) and the experimental result by (Ex) are comparable and the experimental results are almost everywhere lower than the calculated ones. Moreover the theoretical buckling load as reported by [19] deduced from [22] is always much greater than the experimental collapse load, it confirms that the collapse of the observed specimens take place without meaningful geometric nonlinearity occurrence. The comparison showed that the proposed method has given accurate results with respect to the experimental and (CL) ones. Moreover, SAM results are almost everywhere comprised between (Ex) and (CL). The behavior of different procedures can be interpreted by considering that the proposed method apply the static approach hence it gives lower bound of the actual collapse load, the analytical approach of [12] is based on the use of crack lines development and mechanism balance so it consists of a kinematic

 doi:10.20944/preprints202208.0076.v1

theorem application, as a consequence it furnishes an upper bound of the collapse load as it can be seen from the graphic in Fig. 9 where the (CL) results are almost everywhere higher than the experiments' results. As it has to be expected because of the theoretical statements, the proposed method gives results that are almost everywhere lower than the (CL). The Semi Analytical method, however, overestimates the experimental results of several specimens since it is a discretized application of the lower bound theorem of the limit analysis, hence it did not guarantee that the compatibility condition is enforced in all the structure but only at the sampling points. As a consequence, the calculated limit load must decrease at the increasing of the number of sampling points, i.e. the number of discrete co-latitude angles where the inequalities in equation (13) are enforced [15].

6. Conclusions

In the proposed work, a comparison between the Semi-Analytical Method developed in [17] with experiments reported in [13] and numerical calculations in [12,19] have been presented. The SAM, whose formulation has been developed for spherical domes of general shape under generic load pattern, has been particularized to slender caps to compare the strategy with experimental results and theoretical methods based on the fracture lines and the kinematic approach. The constitutive law and the corresponding limit domain of the structural material have been derived considering the Not Tensile Resistant Material model of the unreinforced concrete like that used for the reference concrete caps in [12,13,19]. The collapse multiplier has been determined by evaluating the existence of a statically admissible state of stress under loads of prescribed intensity. The statically admissible stress state consisted of the sum of the semi-analytical solution of the balance equation of spherical domes and the simple linearly elastic solution under the prescribed load obtained through finite element linear solution. The comparison with experimental results and the simplest closed-form solution of domes under radial pressures showed that the method could predict the collapse load accurately. It has to be highlighted that the method can be applied to spherical domes under axial-symmetrical loads quite general; moreover, it can be applied to randomly variable loads to get the shakedown limit of the structures without any complications. The method requires the knowledge of linearly elastic solution under the prescribed loads; this solution can be derived from a closed-form one if it exists or from any numerical solution obtained through well-established methods. However, it must be stressed that the required elastic solution is obtained only using linearly elastic methods and does not require any iterative ultra elastic calculation. Remember that when the collapse multiplier for a prescribed load path must be numerically calculated, one has to apply iterative strategy, and nonlinear plasticity constitutive laws; the latter consisting not only of a limit domain but also of the flow rule that influences the calculation effort and the computational time [23]. Finally, the proposed procedure also calculates the structure's Melan residuals and the compatible stress distribution at the incoming collapse that can be used to calculate the upper bounds of the plastic dissipation at the collapse [18]. In conclusion, the results obtained in the present work have been at first compared with the analytical solution proposed by [19] and then with the numerical experiment proposed by [13]. The proposed method demonstrates its ability to get the load multiplier with no assumptions about the collapse mechanism. The independence from the collapse mechanism knowledge is another relevant advantage of such a static approach that allows formulating the limit equilibrium of the structures with no *a priori* intuition of kinematics and collapse shape.

Author Contributions: Conceptualization, R.Z. and V.M; methodology, V.M.; software, V.M. and R.Z.; validation, R.Z., V.M. and L.E.; formal analysis, V.M.; investigation, R.Z., S.P., L.E., E.T. and V.M.; resources, V.M.; data curation, R.Z., S.P. and L.E.; writing—original draft preparation, R.Z.; writing—review and editing, R.Z. and V.M.; visualization, R.Z., V.M. and L.E.; supervision, V.M.; project administration, V.M.; funding acquisition, V.M. All authors have read and agreed to the published version of the manuscript.

Funding: This research was funded by the Università degli Studi della Campania 'L Vanvitelli', grant Programma VALERE: 'VAnviteLli pEr la RicErca', DDG n. 516-24/05/2018.

Institutional Review Board Statement: Not applicable.

Informed Consent Statement: Not applicable.

Data Availability Statement: Not applicable.

Conflicts of Interest: The authors declare no conflict of interest.

References

1. Block, P.; Ciblac, T.; Ochsendorf, J. Real-time limit analysis of vaulted masonry buildings. *Computers and Structures* **2006**, *84*, 1841–1852. https://doi.org/10.1016/j.compstruc.2006.08.002.
2. Block, P.; Ochsendorf, J. Thrust network analysis: A new methodology for three-dimensional equilibrium. *Journal of the International Association for Shell and Spatial Structures* **2007**, *48*.
3. Block, P.; Lachauer, L. Three-dimensional (3D) equilibrium analysis of gothic masonry vaults. *International Journal of Architectural Heritage* **2014**, *8*. https://doi.org/10.1080/15583058.2013.826301.
4. Avelino, R.M.; Iannuzzo, A.; Mele, T.V.; Block, P. Assessing the safety of vaulted masonry structures using thrust network analysis. *Computers and Structures* **2021**, *257*. https://doi.org/10.1016/j.compstruc.2021.106647.
5. Save, M. Limit analysis and design of containment vessels. *Nuclear Engineering and Design* **1984**, *79*. https://doi.org/10.1016/0029-5493(84)90048-7.
6. Moncarz, P.D.; Griffith, M.; Noakowski, P. Collapse of a Reinforced Concrete Dome in a Wastewater Treatment Plant Digester Tank. *Journal of Performance of Constructed Facilities* **2007**, *21*. https://doi.org/10.1061/(asce)0887-3828(2007)21:1(4).
7. Teng, J.G.; Rotter, J.M. Geometrically and materially nonlinear analysis of reinforced concrete shells of revolution. *Computers and Structures* **1992**, *42*. https://doi.org/10.1016/0045-7949(92)90029-Y.
8. Zingoni, A.; Enoma, N. Strength and stability of spherical-conical shell assemblies under external hydrostatic pressure. *Thin-Walled Structures* **2020**, *146*. https://doi.org/10.1016/j.tws.2019.106472.
9. Zingoni, A. Stress and buckling resistance of dual-purpose concrete shells. *Thin-Walled Structures* **2022**, *170*. https://doi.org/10.1016/j.tws.2021.108596.
10. Stockdale, G.; Milani, G. Diagram based assessment strategy for first-order analysis of masonry arches. *Journal of Building Engineering* **2019**, *22*, 122–129. https://doi.org/10.1016/j.jobe.2018.12.002.
11. Mercuri, M.; Pathirage, M.; Gregori, A.; Cusatis, G. Masonry vaulted structures under spreading supports: Analyses of fracturing behavior and size effect. *Journal of Building Engineering* **2022**, *45*. https://doi.org/10.1016/j.jobe.2021.103396.
12. Chang, Z.T.; Bradford, M.A.; Gilbert, R.I. Short-term behaviour of shallow thin-walled concrete dome under uniform external pressure. *Thin-Walled Structures* **2011**, *49*. https://doi.org/10.1016/j.tws.2010.08.012.
13. Vandepitte, D.; Lagae, G. Buckling of Spherical Domes Made of Microconcrete and Creep Buckling of Such Domes Under Long-term Loading. In Proceedings of the Inelastic Behaviour of Plates and Shells; Bevilacqua, L.; Feijóo, R.; Valid, R., Eds.; Springer Berlin Heidelberg: Berlin, Heidelberg, 1986; pp. 291–311.
14. Zoelly, R. *Uber ein Knickungs problem an der Kugelschale, PhD Thesis*; ETH Druck von Zurker & Furrer, 1915.
15. Palladino, S.; Esposito, L.; Ferla, P.; Totaro, E.; Zona, R.; Minutolo, V. Experimental and numerical evaluation of residual displacement and ductility in ratcheting and shakedown of an aluminum beam. *Applied Sciences (Switzerland)* **2020**, *10*.
16. Zona, R.; Esposito, L.; Ferla, P.; Palladino, S.; Totaro, E.; Minutolo, V. Lower bound limit analysis of parabolic domes based on spherical analytical solution. *International Journal of Advanced Research in Engineering and Technology* **2020**, *11*, 59–79. https://doi.org/10.34218/IJARET.11.6.2020.007.
17. Zona, R.; Ferla, P.; Minutolo, V. Limit analysis of conical and parabolic domes based on semi-analytical solution. *Journal of Building Engineering* **2021**, *44*. https://doi.org/10.1016/j.jobe.2021.103271.
18. Lubliner, J.; Moran, B. Plasticity Theory. *Journal of applied mechanics* **1992**.
19. Chang, Z.T.; Bradford, M.A.; Gilbert, R.I. Limit analysis of local failure in shallow spherical concrete caps subjected to uniform radial pressure. *Thin-Walled Structures* **2010**, *48*. https://doi.org/10.1016/j.tws.2010.01.014.
20. Timoshenko, S.P. *Theory of Plates and Shells*, 1 ed.; Vol. 1, McGraw-Hill, 1964.
21. Heyman, J. The stone skeleton. *International Journal of Solids and Structures* **1966**, *2*.
22. O'Dwyer, D. Funicular analysis of masonry vaults. *Computers and Structures* **1999**, *73*, 187–197. https://doi.org/10.1016/S0045-7949(98)00279-X.
23. Clementi, F.; Gazzani, V.; Poiani, M.; Lenci, S. Assessment of seismic behaviour of heritage masonry buildings using numerical modelling. *Journal of Building Engineering* **2016**, *8*, 29–47. https://doi.org/10.1016/j.jobe.2016.09.005.